Natural convection instability during carbon dioxide storage into deep saline aquifers

A.K. Singh[1], W. Wang[1], U.-J. Görke[1], and O. Kolditz[1,2]

Processes

- Fluid mass balance equation of water and vapor

$$\frac{\partial[\phi(1-S_w)\rho_{gw}]}{\partial t}-\nabla\cdot\left[\rho_{gw}\frac{\mathbf{k}k_{rg}}{\mu_g}\nabla p_g\right]-\nabla\cdot\left[\rho_g\frac{M_aM_w}{M_g^2}\mathbf{D}_{eff}\nabla\left(\frac{p_{gw}}{p_g}\right)\right]=-\frac{\partial[\phi S_w\rho_w]}{\partial t}+\nabla\cdot\left[\rho_w\frac{\mathbf{k}k_{rw}}{\mu_w}\nabla p_w\right]$$

- Fluid mass balance equation of CO_2

$$\frac{\partial[\phi(1-S_w)\rho_{ga}]}{\partial t}-\nabla\cdot\left[\rho_{ga}\frac{\mathbf{k}k_{rg}}{\mu_g}\nabla p_g\right]+\nabla\cdot\left[\rho_g\frac{M_aM_w}{M_g^2}\mathbf{D}_{eff}\nabla\left(\frac{p_{gw}}{p_g}\right)\right]=0$$

- Energy balance equation

$$(\rho c_p)_{eff}\frac{\partial T}{\partial t}-\left[\rho_w c_{pw}\frac{\mathbf{k}k_{rw}}{\mu_w}\nabla p_w+\rho_g c_{pg}\frac{\mathbf{k}k_{rg}}{\mu_g}\nabla p_g\right]\cdot\nabla T-\nabla\cdot[\boldsymbol{\kappa}_{eff}\nabla T]=\Delta H_{VAP}\left(\frac{\partial[\phi S_w\rho_w]}{\partial t}-\nabla\cdot\left[\rho_w\frac{\mathbf{k}k_{rw}}{\mu_w}\nabla p_w\right]\right)\rightarrow\dot{m}_{vap}$$

$$(\rho c_p)_{eff}=\phi S_w\rho_w c_{pw}+\phi(1-S_w)\rho_g c_{pg}+(1-\phi)\rho_s c_{ps}$$

$$\kappa_{eff}=\phi S_w\kappa_w+\phi(1-S_w)\kappa_g+(1-\phi)\kappa_s$$

EOS

Fluid Properties

Meaning	Ref	Unit
Water density	$\rho_w=\rho_{w0}\cdot[1-\beta_T\cdot(T-T_0)]$	$kg\cdot m^{-3}$
Gas density	$\rho_g=\frac{M_w\cdot P_{gw}+M_a\cdot P_{ga}}{R\cdot T}$	$kg\cdot m^{-3}$
Water viscosity	$\mu_w=a+b\cdot T+c\cdot T^2+d\cdot T^3$	$Pa\cdot s$
Gas viscosity	$\mu_g=x_{gw}\cdot\mu_{gw}+x_{ga}\cdot\mu_{ga}$	$Pa\cdot s$
Water heat capacity	$c_{pw}=a+b\cdot T+c\cdot T^2$	$J\cdot kg^{-1}\cdot K^{-1}$
Gas heat capacity	$c_{pg}=x_{gw}\cdot c_{pgw}+x_{ga}\cdot c_{pga}$	$J\cdot kg^{-1}\cdot K^{-1}$
Water conductivity	$c_{pw}=a+b\cdot T+c\cdot T^2$	$W\cdot m^{-1}\cdot K^{-1}$
Gas conductivity	$\kappa_g=x_{gw}\cdot\kappa_{gw}+x_{ga}\cdot\kappa_{ga}$	$W\cdot m^{-1}\cdot K^{-1}$
Enthalpy of vaporization	$\Delta H_{VAP}=2.6673\times10^5\cdot(T_{cr}-T)^{0.38}$	$J\cdot kg^{-1}$
Saturated vapor pressure	$P_{gw}=P_{gw0}\cdot e^{\left[\frac{-M_w\Delta H_{VAP}}{T}\left(\frac{1}{T}-\frac{1}{T_0}\right)\right]}$	Pa
Vapor pressure	$P_{gw}=P_{gw}\cdot e^{\left(\frac{M_wP_c}{\rho_wRT}\right)}$	Pa
Effective diffusion coefficient	$D_{eff}=\tau\cdot(1-S_w)\cdot2.16\times10^5\cdot\left(\frac{T}{T_{dat}}\right)^{1.8}$	$m^2\cdot s^{-1}$
Surface tension	$\sigma=0.3258\cdot\chi^{1.256}-0.3258\cdot\chi^{2.256}$; $\chi=\left(1-\frac{T}{647.3}\right)$	$kg\cdot s^{-2}$
Vapor fraction	$x_{gw}=\frac{\rho_{gw}}{\rho_g}$	

Numerical schemes

Weighted residuals for the weak form, spatially discretized based on Galerkin approach (hybrid monolithic/staggered scheme).

$$M_\psi\ \dot{\psi}+(A_\psi+K_\psi)\ \psi=f_\psi \text{ and } M_T\ \dot{T}+(A_T+K_T)\ T=f_T$$

where $\psi=(p,p_c)^{tr}$ stands for gas and capillary pressure unknowns at element nodes.

Generalized single step time discretization scheme.

$$[M+\theta\Delta t(A+K)]\xi^{m+1}=[M-(1-\theta)\Delta t(A+K)]\xi^m,\ \text{With}\ \theta\ \geq0.5$$

- Primary variables: gas pressure, capillary pressure and temperature
- Monolithic scheme for pressure and capillary pressure
- Staggered scheme for temperature
- Coupling terms calculated at each Gauss point by interpolating nodal values
- Picard linearization for nonlinear iterations

Benchmark

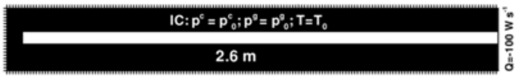

Benchmark sketch.

- The test benchmark problem for heat pipe effects is formulated in 1D column is filled with fluid subjected to heat flux q_T=100, at the right end where left end temperature maintained below to the saturation temperature
- Pressure gradients are derived for each phases in two-phase flow with heat transfer. Then obtained saturation gradient is integrated over two-phase regime. Two-phase zone is defined by imposing the limits of integration on saturation, i.e. S=S_0 at x=0 and S= S_1 at x=L. L is length of two phase zone.
- Decrease in vapour density is described by Kelvin equation and divergent form of temperature is obtained by using pressure gradients
- Coupled differential equations are integrated by using Euler method with following boundary conditions at x = 0: S=S_0. p_g=p_{g0}, pc = p_{c0} and T=T_{sat}
- The scientific open source code OpenGeoSys for multi-phase flow is used for simulation

Geometry and material parameters.

Meaning	Symbol	Value	Unit
Column length	L	2.6	m
Solid density	ρ_s	2560	kg m^{-3}
Solid heat capacity	c_{ps}	1200	J kg^{-1} K^{-1}
Solid thermal conductivity	κ_s	2.5	W m^{-1} K^{-1}
Intrinsic permeability	**k**	1.0x10-13	m^2
Porosity	φ	0.35	-
Residual saturation	$S_{rw'}$	0.2	-
Distribution index	λ	2	-
Entry pressure	p_d	Brooks Corey	Pa
Relative permeability	k_r	Brooks Corey	-

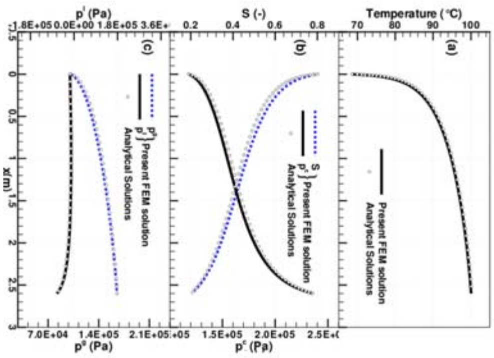

Profiles of primary variable are compared with analytical solution for heat pipe example.

- Obtained solution for primary variables are well matched with the analytical solution
- Deviation at saturation distribution is due to saturation obtained by interpolating over gauss point
- The numerical model is implemented in the framework of the open source scientific software OpenGeoSys (OGS)
- OGS is based on object-oriented programming principles allowing model applications in various geotechnical areas

Application

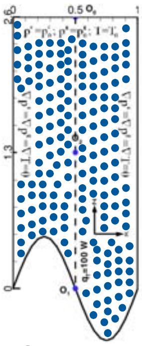

System geometry and boundary conditions.

- Two-phase natural convection and instability analysis by quality is presented for CCS into deep saline aquifers
- We assume that the aquifer is a partially saturated with CO_2 and water
- Potential two-phase flow instability, i.e. thermal oscillations is encountered. This is important for design and operation of CCS
- Structure and stability of the two-phase mixed convection process is characterized by N_{sub} and N_{Pch}
- Identical N_{sub} and N_{Pch} represent similar quality (x_{eg}) development of the flow.

Two numbers are defined as follow

$$N_{Pch}=\frac{(\rho_w-\rho_g)q_T}{\rho_g\dot{m}_{vap}\Delta H_{vap}}\ \text{and}\ N_{Sub}=\frac{(\rho_w-\rho_g)c_{pw}\Delta T}{\rho_g\Delta H_{vap}}$$

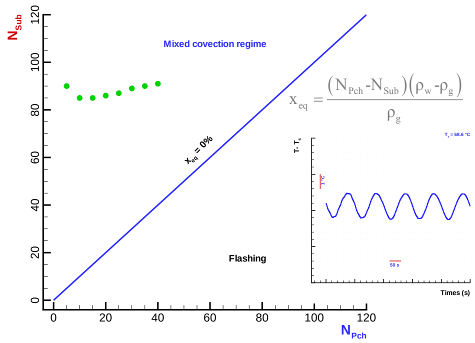

Operational stability diagram and thermal oscillations.

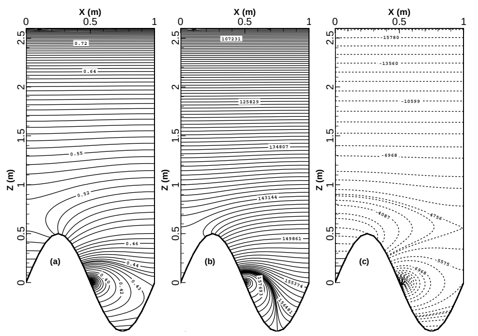

Distribution of the time averaged (a) saturation; (b) vapor pressure ; (c) water pressure.

Conclusions

- Thermal oscillations occur at heat flux at q_T=100 Wm^{-2} , moreover its aplitude is depending on heat input
- Here, N_{Sub} and N_{Pch} are identical and qualit x_{eq} = 0% showing stable two-phase flow.

Acknowledgement

The authors acknowledge the funding by the German Federal Ministry of Education and Research (BMBF) within the framework of CO2 related joint projects as parts of the Special Program GEOTECHNOLOGIEN.

Contact:

1) Department of Environmental Informatics, Helmholtz Centre for Environmental Research – UFZ, Permoserstr. 15, D-04318 Leipzig, Germany, ashok.singh@ufz.de

2) Environmental System Analysis, TU Dresden

HELMHOLTZ CENTRE FOR ENVIRONMENTAL RESEARCH – UFZ